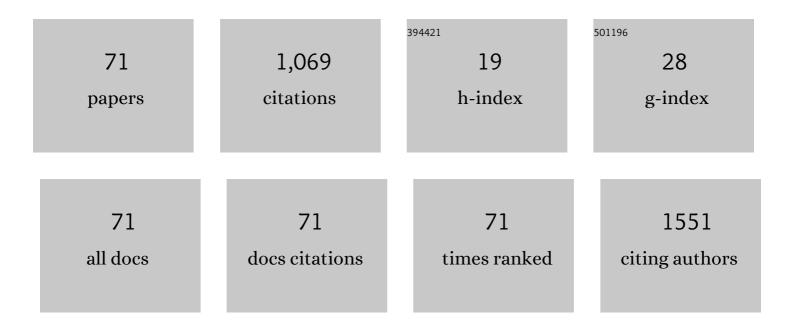
List of Publications by Year in descending order

Source: https://exaly.com/author-pdf/9106854/publications.pdf Version: 2024-02-01



| # | Article | IF | CITATIONS |
|----|---|------|-----------|
| 1 | High Visible Photoelectrochemical Activity of Ag Nanoparticle-Sandwiched CdS/Ag/ZnO Nanorods. ACS Applied Materials & Interfaces, 2017, 9, 658-667. | 8.0 | 86 |
| 2 | Highly transparent and conductive Al-doped ZnO films synthesized by pulsed laser co-ablation of Zn and Al targets assisted by oxygen plasma. Journal of Alloys and Compounds, 2015, 626, 415-420. | 5.5 | 50 |
| 3 | Blue shift in absorption edge and widening of band gap of ZnO by Al doping and Al–N co-doping. Journal of Alloys and Compounds, 2015, 644, 528-533. | 5.5 | 49 |
| 4 | Photoluminescence and low-threshold lasing of ZnO nanorod arrays. Optics Express, 2012, 20, 14857. | 3.4 | 37 |
| 5 | Enhanced Photoelectrochemical Activity of ZnO-Coated TiO2 Nanotubes and Its Dependence on ZnO Coating Thickness. Nanoscale Research Letters, 2016, 11, 104. | 5.7 | 35 |
| 6 | Photoluminescence and Lasing Properties of Catalyst-Free ZnO Nanorod Arrays Fabricated by Pulsed Laser Deposition. Journal of Physical Chemistry C, 2012, 116, 2330-2335. | 3.1 | 33 |
| 7 | Controlled growth of crystalline g-C3N4 nanocone arrays by plasma sputtering reaction deposition. Carbon, 2014, 79, 578-589. | 10.3 | 33 |
| 8 | Manipulations from oxygen partial pressure on the higher energy electronic transition and dielectric function of VO ₂ films during a metal–insulator transition process. Journal of Materials Chemistry C, 2015, 3, 5033-5040. | 5.5 | 33 |
| 9 | Radio-frequency epsilon-negative property and diamagnetic response of percolative Ag/CCTO metacomposites. Scripta Materialia, 2021, 203, 114067. | 5.2 | 33 |
| 10 | Enhanced photoelectrochemical activity of vertically aligned ZnO-coated TiO2 nanotubes. Applied Physics Letters, 2014, 104, 053114. | 3.3 | 31 |
| 11 | Graphene–Carbon Black/CaCu ₃ Ti ₄ O ₁₂ Ternary Metacomposites toward a Tunable and Weakly ε-Negative Property at the Radio-Frequency Region. Journal of Physical Chemistry C, 2020, 124, 23361-23367. | 3.1 | 30 |
| 12 | Arsenic doping for synthesis of nanocrystalline p-type ZnO thin films. Journal of Vacuum Science and Technology A: Vacuum, Surfaces and Films, 2006, 24, 517-520. | 2.1 | 27 |
| 13 | Enhanced charge separation of vertically aligned CdS/g-C ₃ N ₄ heterojunction nanocone arrays and corresponding mechanisms. Journal of Materials Chemistry C, 2016, 4, 7501-7507. | 5.5 | 26 |
| 14 | Extended photoresponse of ZnO/CdS core/shell nanorods to solar radiation and related mechanisms. Solar Energy Materials and Solar Cells, 2015, 137, 169-174. | 6.2 | 25 |
| 15 | Tailoring of optical and electrical properties of transparent and conductive Al-doped ZnO films by adjustment of Al concentration. Materials Science in Semiconductor Processing, 2018, 74, 147-153. | 4.0 | 23 |
| 16 | The electro-optic mechanism and infrared switching dynamic of the hybrid multilayer VO2/Al:ZnO heterojunctions. Scientific Reports, 2017, 7, 4425. | 3.3 | 20 |
| 17 | ZnO colloids and ZnO nanoparticles synthesized by pulsed laser ablation of zinc powders in water. Materials Science in Semiconductor Processing, 2020, 109, 104918. | 4.0 | 20 |
| 18 | Photoluminescence and its time evolution of AlN thin films. Physics Letters, Section A: General, Atomic and Solid State Physics, 2001, 280, 381-385. | 2.1 | 19 |

| # | Article | IF | CITATIONS |
|----|--|-----|-----------|
| 19 | Growth of ZnSe nanowires by pulsed-laser deposition. Journal of Vacuum Science & Technology B, 2007, 25, 1823. | 1.3 | 19 |
| 20 | Study on phase separation in a-SiOx for Si nanocrystal formation through the correlation of photoluminescence with structural and optical properties. Applied Surface Science, 2011, 257, 6145-6151. | 6.1 | 19 |
| 21 | Extended photoresponse and multi-band luminescence of ZnO/ZnSe core/shell nanorods. Nanoscale Research Letters, 2014, 9, 31. | 5.7 | 19 |
| 22 | Extended photo-response of ZnO/CdS core/shell nanorods fabricated by hydrothermal reaction and pulsed laser deposition. Optics Express, 2014, 22, 8617. | 3.4 | 17 |
| 23 | Engineering of optical and electrical properties of ZnO by non-equilibrium thermal processing: The role of zinc interstitials and zinc vacancies. Journal of Applied Physics, 2017, 122, 035303. | 2.5 | 17 |
| 24 | WS2 coating and Au nanoparticle decoration of ZnO nanorods for improving light-activated NO2 sensing. Applied Surface Science, 2022, 584, 152508. | 6.1 | 16 |
| 25 | Optoelectronic properties of ZnO film on silicon after SF ₆ plasma treatment and milliseconds annealing. Applied Physics Letters, 2014, 105, 221903. | 3.3 | 15 |
| 26 | Enhanced visible photoelectrochemical properties of ZnO/CdS core/shell nanorods and their correlation with improved optical properties. Applied Physics Letters, 2016, 109, 203106. | 3.3 | 15 |
| 27 | ZnO:Au nanocomposites with high photocatalytic activity prepared by liquid-phase pulsed laser ablation. Optics and Laser Technology, 2021, 133, 106533. | 4.6 | 15 |
| 28 | A comparative study of the enhancement of molecular emission in a spatially confined plume through optical emission spectroscopy and probe beam deflection measurements. Spectrochimica Acta, Part B: Atomic Spectroscopy, 2013, 79-80, 44-50. | 2.9 | 14 |
| 29 | Spectroscopic characterization of the plasmas formed during the deposition of ZnO and Al-doped ZnO films by plasma-assisted pulsed laser deposition. Spectrochimica Acta, Part B: Atomic Spectroscopy, 2016, 125, 18-24. | 2.9 | 13 |
| 30 | Spectral assignments in the infrared absorption region and anomalous thermal hysteresis in the interband electronic transition of vanadium dioxide films. Physical Chemistry Chemical Physics, 2016, 18, 6239-6246. | 2.8 | 13 |
| 31 | Sandwiched CdS/Au/ZnO Nanorods with Enhanced Ultraviolet and Visible Photochemical and Photoelectrochemical Properties via Semiconductor and Metal Cosensitizing. Journal of Physical Chemistry C, 2020, 124, 10941-10950. | 3.1 | 13 |
| 32 | Fabrication and correlation between photoluminescence and photoelectrochemical properties of vertically aligned ZnO coated TiO2 nanotube arrays. Solar Energy Materials and Solar Cells, 2014, 123, 233-238. | 6.2 | 12 |
| 33 | Size-controllable growth of ZnO nanorods on Si substrate. Superlattices and Microstructures, 2017, 101, 469-479. | 3.1 | 12 |
| 34 | Correlation between structure and photoluminescence of c-axis oriented nanocrystalline ZnO films and evolution of photo-generated excitons. Solar Energy Materials and Solar Cells, 2012, 96, 117-123. | 6.2 | 11 |
| 35 | Enhancement and stability of photoluminescence from Si nanocrystals embedded in a SiO2 matrix by H2-passivation. Applied Surface Science, 2014, 300, 178-183. | 6.1 | 11 |
| 36 | Multi-band luminescent ZnO/ZnSe core/shell nanorods and their temperature-dependent photoluminescence. RSC Advances, 2016, 6, 98413-98421. | 3.6 | 11 |

| # | Article | IF | CITATIONS |
|----|--|-----|-----------|
| 37 | CuO: Synthesis in a Highly Excited Oxygen-Copper Plasma and Decoration of ZnO Nanorods for Enhanced Photocatalysis. Journal of Physical Chemistry C, 2021, 125, 9119-9128. | 3.1 | 11 |
| 38 | Infrared and Raman Spectroscopic Studies of Optically Transparent Zirconia (ZrO ₂) Films Deposited by Plasma-Assisted Reactive Pulsed Laser Deposition. Applied Spectroscopy, 2011, 65, 522-527. | 2.2 | 10 |
| 39 | Composition and bandgap control of Al _x Ga _{1â^'x} N films synthesized by plasma-assisted pulsed laser deposition. Journal of Materials Chemistry C, 2015, 3, 5307-5315. | 5.5 | 10 |
| 40 | Confinement effects of shock waves on laser-induced plasma from a graphite target. Physics of Plasmas, 2015, 22, 063509. | 1.9 | 10 |
| 41 | Synthesis and characterization of single-crystalline graphitic C ₃ N ₄ nanocones. CrystEngComm, 2015, 17, 512-515. | 2.6 | 10 |
| 42 | Annealing behaviors of structural, interfacial and optical properties of HfO2 thin films prepared by plasma assisted reactive pulsed laser deposition. Journal of Materials Research, 2010, 25, 680-686. | 2.6 | 9 |
| 43 | Growth of CdS Nanoneedles by Pulsed Laser Deposition. Journal of Electronic Materials, 2012, 41, 1941-1947. | 2.2 | 9 |
| 44 | Synthesis, phase transition and optical properties of nanocrystalline titanium dioxide films deposited by plasma assisted reactive pulsed laser deposition. Surface and Coatings Technology, 2013, 231, 180-184. | 4.8 | 9 |
| 45 | ZnS Covering of ZnO Nanorods for Enhancing UV Emission from ZnO. Journal of Physical Chemistry C, 2021, 125, 13732-13740. | 3.1 | 9 |
| 46 | Growth of Nanocrystalline ZnSe:N Films by Pulsed Laser Deposition. Journal of Electronic Materials, 2007, 36, 75-80. | 2.2 | 8 |
| 47 | Photoluminescence enhancement of Si nanocrystals embedded in SiO2 by thermal annealing in air. Applied Surface Science, 2014, 320, 804-809. | 6.1 | 8 |
| 48 | Polycrystalline ZnTe thin film on silicon synthesized by pulsed laser deposition and subsequent pulsed laser melting. Materials Research Express, 2016, 3, 036403. | 1.6 | 8 |
| 49 | Spatial confinement of laser-induced plasma by laser-induced and obstacle-reflected shock wave and its effect on optical emission of laser-induced plasma. AIP Advances, 2019, 9, . | 1.3 | 7 |
| 50 | Raman spectra of nanocrystalline carbon nitride synthesized on cobalt-covered substrate by nitrogen-atom-beam-assisted pulsed laser ablation. Journal of Applied Physics, 2002, 92, 496-500. | 2.5 | 6 |
| 51 | High excitation of the species in nitrogen–aluminum plasma generated by electron cyclotron resonance microwave discharge of N2 gas and pulsed laser ablation of Al target. Spectrochimica Acta, Part B: Atomic Spectroscopy, 2014, 101, 226-233. | 2.9 | 6 |
| 52 | Large Enhancement and Its Mechanism of Ultraviolet Emission from ZnO Nanorod Arrays at Room and Low Temperatures by Covering with Ti Coatings. Journal of Physical Chemistry C, 2020, 124, 4827-4834. | 3.1 | 6 |
| 53 | Synthesis of Plasmonic Z-Scheme g-C3N4/W18O49 Nanocone Arrays with Enhanced Charge Separation. Journal of Physical Chemistry C, 2021, 125, 4205-4210. | 3.1 | 6 |
| 54 | Auâ€Decorated ZnO Nanorod Powder and Its Application in Photodegradation of Organic Pollutants in the Visible Region. Physica Status Solidi (A) Applications and Materials Science, 2021, 218, 2000737. | 1.8 | 6 |

| # | Article | IF | CITATIONS |
|----|---|-----|-----------|
| 55 | WS2-decorated ZnO nanorods and enhanced ultraviolet emission. Materials Letters, 2022, 306, 130880. | 2.6 | 6 |
| 56 | Synthesis of carbon nitride nanocrystals on Co/Ni-covered substrate by nitrogen-atom-beam-assisted pulsed laser ablation. Journal of Materials Research, 2003, 18, 2552-2555. | 2.6 | 5 |
| 57 | Self-Assembled Fabrication and Characterization of Vertically Aligned Binary CN Nanocone Arrays. Journal of Electronic Materials, 2010, 39, 381-390. | 2.2 | 5 |
| 58 | Formation of diatomic molecular radicals in reactive nitrogen-carbon plasma generated by electron cyclotron resonance discharge and pulsed laser ablation. Physics of Plasmas, 2014, 21, 043512. | 1.9 | 5 |
| 59 | Enhanced light absorption and quenched photoluminescence resulting in photoactive poly(3-hexyl-thiophene)-covered ZnO/TiO 2 nanotubes for high light harvesting efficiency. Solar Energy Materials and Solar Cells, 2017, 162, 47-54. | 6.2 | 5 |
| 60 | Highâ€Visibleâ€Light Photocatalytic Activity of ZnO–Au Nanocomposites Synthesized by a Controlled Hydrothermal Method. Physica Status Solidi (A) Applications and Materials Science, 2021, 218, 2100150. | 1.8 | 5 |
| 61 | Spectroscopic Characterization of Plasmas Generated by ECR Microwave Discharge of N ₂ Gas and Pulsed Laser Ablation of a B ₄ C Target. Plasma Processes and Polymers, 2011, 8, 1146-1153. | 3.0 | 4 |
| 62 | Evolution of photoluminescence from Si nanocrystals embedded in a SiO ₂ matrix prepared by reactive pulsed laser deposition. Journal of Materials Research, 2009, 24, 2259-2267. | 2.6 | 3 |
| 63 | Ab initio calculation of diffusion barriers for Cu adatom hopping on Cu(100) surface and evolution of atomic configurations. Applied Surface Science, 2011, 257, 7507-7515. | 6.1 | 2 |
| 64 | Transparent polycrystalline monoclinic HfO2 dielectrics prepared by plasma assisted pulsed laser deposition. Journal of Vacuum Science and Technology A: Vacuum, Surfaces and Films, 2012, 30, 011506. | 2.1 | 2 |
| 65 | Effects of the experimental conditions on the growth of crystalline NiCx nanorods via pulsed laser deposition accompanied by N2 annealing. Applied Surface Science, 2017, 403, 670-676. | 6.1 | 2 |
| 66 | Structure and optical properties of ZrxHf1-xO2 films deposited by pulsed laser co-ablation of Zr and Hf targets with the assistance of oxygen plasma. Ceramics International, 2021, 48, 587-587. | 4.8 | 2 |
| 67 | Spectroscopic characterization of the plasma generated during the deposition of Al _{<i>x</i>} Ga _{1â~'<i>x</i>} N films by pulsed laser co-ablation of Al and GaAs targets in electron cyclotron resonance nitrogen plasma. Journal Physics D: Applied Physics, 2015, 48, 245203. | 2.8 | 1 |
| 68 | Spectroscopic studies of the plasma for the preparation of Al-N co-doped ZnO films. Spectrochimica Acta, Part B: Atomic Spectroscopy, 2017, 131, 48-57. | 2.9 | 1 |
| 69 | Effects of experimental conditions on the growth of g–C ₃ N ₄ nanocones by plasma sputtering reaction deposition. Functional Materials Letters, 2022, 15, . | 1.2 | 1 |
| 70 | Structure and photoluminescence of c-axis oriented Nnanocrystalline ZnO films synthesized by plasma assisted pulsed laser deposition. , 2010, , . | | 0 |
| 71 | Optical Properties of ZnO Nanorod-Based Heterogeneous Core/Shell Arrays. , 2015, , . | | 0 |